

CO₂ Reforming of CH₄ over Pt/ZrO₂ Catalysts Promoted with La and Ce Oxides

Susan M. Stagg-Williams,¹ Fabio B. Noronha, Gene Fendley, and Daniel E. Resasco²

School of Chemical Engineering and Materials Science, and Institute for Gas Utilization Technologies, University of Oklahoma, 100 East Boyd Street, Norman, Oklahoma 73019

Received December 17, 1999; revised May 22, 2000; accepted May 31, 2000

INTRODUCTION

The CO₂ reforming of CH₄ was studied over cerium- and lanthanum-promoted Pt/ZrO₂ catalysts at 1073 K and a CH₄:CO₂ ratio of 2:1. The high ratios of CH₄:CO₂ were used in an attempt to accelerate deactivation of the catalyst and make a faster comparison of the different samples. The addition of Ce resulted in a significant improvement in the stability, with no decrease in either CH₄ or CO₂ conversion observed. The promotion with La also resulted in an increase in the stability of the catalyst as well as an increase in the initial activity. The mechanism of reaction has been studied on the promoted catalysts, and it has been shown that it is not altered by the presence of the promoters. The long-term activity of the catalyst is dependent upon the balance between the rate of CH₄ decomposition and the rate of dissociation of CO₂. The results of pulse studies demonstrate that addition of the cerium results in an increase in the reducibility and oxygen transfer ability of the support. Temperature-programmed oxidation studies demonstrated that although the total amount of carbon deposits on the Ce-promoted catalyst is not lower than that on the unpromoted one, these deposits are eliminated at much lower temperature, indicating the ability of the catalyst to clean the active sites. On the other hand, the TPO studies on the La-doped catalyst showed a much lower extent of carbon deposition. Interestingly, the ability of La to inhibit carbon formation is only observed in the presence of CO₂. Under pulses of pure CH₄, the La-promoted catalyst was the one which showed the highest tendency for carbon deposition. X-ray diffraction and BET area characterization of this catalyst showed that the promoter increases the thermal stability of the support. Finally, it was shown that the promoters also retard metal particle growth during reaction at high temperature. Smaller Pt particles result in an increase in the interfacial area and subsequent increase in the removal of the carbon from the metal. The increase in the efficiency of the cleaning mechanism resulted in catalysts that were stable for the dry reforming reaction under severely deactivating conditions (i.e., 1073 K, CH₄:CO₂ ratio = 2:1) for over 20 h.

© 2000 Academic Press

Methane reforming using carbon dioxide (dry reforming) has been of interest for many years (1–3), but recently that interest has experienced a rapid increase for both environmental and commercial reasons. One potential advantage of dry reforming that would have an impact on the industrial sector is the lower H₂:CO product ratio that can be produced, i.e., 1:1 or less. A lower H₂:CO ratio (compared to steam reforming and partial oxidation) is preferred for the production of oxygenated compounds (4, 5), and it also introduces the possibility of combining the steam reforming, partial oxidation, and dry reforming reactions to get the desired H₂:CO ratio (6–8). Furthermore, the use of CO₂ provides a source of clean oxygen, which eliminates the need for costly separation plants, which are necessary for partial oxidation. An additional, and perhaps most important, advantage of dry reforming is in those cases in which the reactants are simultaneously available at low cost, or even at negative prices (9, 10). Natural gas reservoirs contain primarily CH₄, but some reservoirs also have a large fraction of CO₂ (11–13). Many of these reservoirs are located in remote regions and have quantities of natural gas that are too small to make production economical. The capability to convert the natural gas in these reservoirs to higher value products in an efficient manner could increase the cost effectiveness of remotely located reservoirs. This capability, along with the other advantages, makes the dry reforming reaction very desirable for commercialization.

The major obstacle preventing commercialization of this process is that, due to the high endothermic nature of the process, temperatures near 1073 K are required to reach high conversions. Under these conditions the catalyst experiences rapid deactivation due to carbon deposition. In several studies (4, 14–19) Pt/ZrO₂ catalysts have been shown to be very stable for the dry reforming reaction when operating at moderate temperatures, 923 K. However, these catalysts also deactivate due to carbon deposition when operating at higher temperatures, 1073 K, and CH₄:CO₂ ratios greater than 1. Previous studies (20) have provided

¹ Current address: Chemical and Petroleum Engineering Department, University of Kansas, 4006 Learned Hall, Lawrence, KS 66045.

² To whom correspondence should be addressed. E-mail: resasco@ou.edu. Fax: (405) 325-5813.

evidence that on the Pt/ZrO₂ catalyst, the decomposition of CH₄ and the dissociation of CO₂ occur via two independent paths. The first path involves the decomposition of CH₄ on the metal particle, resulting in the formation of H₂. Carbon formed during the decomposition of CH₄ can partially reduce the oxide support near the metal particle or, in the absence of a reducible oxide, form carbon deposits on the metal. The second path is the dissociation of CO₂. The CO₂ adsorbs on the support and, when near the metal particle, dissociates to form CO and O. The oxygen formed during the dissociation can then reoxidize the support to provide a redox mechanism for continuous cleaning. The balance between the rate of decomposition and the rate of cleaning determines the overall stability of the catalyst.

Previous studies have shown that the addition of promoters to the ZrO₂ support results in increased activity and stability for the reforming reaction (21, 22). It is well established that the addition of Y or La oxides enhances the surface area and the thermal stability of ZrO₂ and other supports (23–25). Similarly, doping cerium oxide with Zr⁴⁺ results in a material with an enhanced thermal resistance. For example, after calcination at 1073 K, the doped material had more than six times the surface area of the unpromoted CeO₂ catalyst (26). Furthermore, it is well known that these materials, as well as ceria-doped zirconia, exhibit good oxygen storage capacities and high thermal stability (27, 28). Several studies have been performed on the redox properties of the CeO₂-doped catalysts (29, 30) and have shown that the redox properties of a Ce_{0.5}Zr_{0.5}O₂ mixed oxide support could be improved by repetitive oxidation/reduction cycles (29, 31). The high reducibility and high thermal stability of the promoted ZrO₂ materials make them very attractive supports for the reforming reaction. In this paper, a study of Pt catalysts supported on both Ce-oxide- and La-oxide-doped ZrO₂ is reported. The activity, thermal stability, and BET surface area of the promoted catalysts have been measured and compared to an unpromoted Pt/ZrO₂ catalyst.

EXPERIMENTAL

The zirconium hydroxide, lanthanum (5 wt%)-doped ZrO₂ and cerium (18 wt%)-doped materials were obtained from Magnesium Elektron Inc. A second Ce-doped ZrO₂ was made by aqueous impregnation of cerium nitrate to the zirconium hydroxide. The incipient wetness of the Zr(OH)₄ was 0.2 cm³/g and the weight percentage of Ce in the final material was 5%. The materials were dried overnight at 383 K, and then calcined at 1073 K for 4 h in stagnant air, prior to the addition of the metal. BET analysis has shown that the surface areas of the supports after calcination at 1073 K for 4 h are 55 m²/gram for the La-ZrO₂, 39 m²/gram for the Ce-ZrO₂ (5 wt%), and 35 m²/gram and for the ZrO₂

support. The Pt/ZrO₂, Pt/La-ZrO₂, and Pt/Ce-ZrO₂ catalysts were prepared by incipient wetness impregnation of an aqueous solution of H₂PtCl₆ · 6H₂O with a Pt loading of 1.5 wt%. The Pt/ZrO₂ catalyst, Pt/Ce-ZrO₂ (5 wt%), Pt/Ce-ZrO₂ (18 wt%), and Pt/La-ZrO₂ catalysts were dried overnight at 383 K, and calcined in air (30 cm³/min) for 2 h at 673 K.

Reactions were performed in a quartz flow reactor with an inner diameter of 0.4 cm and an outer diameter of 0.6 cm. Prior to reaction, 10 mg of catalyst was reduced *in situ* in H₂ (30 cm³/min) at 773 K for 1 h and then heated to 1073 K in He (15 cm³/min). The reactions were performed at 1073 K with a CH₄:CO₂ ratio of 2:1 and a flow rate of 150 cm³/min. The conditions were chosen to ensure that the reaction was not operating near equilibrium conditions. A ratio of CH₄:CO₂ higher than that at which one would normally operate in a commercial process (e.g., 1:1) was used in order to accelerate the deactivation of the catalyst. The Weisz-Prater criteria for internal diffusion was calculated, and the results showed that mass transfer limitations were not present in any of the experiments. The exit gases were analyzed using a gas chromatograph (Hewlett Packard HP5890) equipped with a thermal conductivity detector and a Supelco Carboxen 1006 PLOT fused capillary column (30 m, 0.53 mm ID), which allowed for separation of H₂, CO, CH₄, and CO₂. The carrier gas used was Ar. Calibration of the GC using varying ratios of the reactants and products resulted in a mol/area ratio for each gas. Quantification of H₂O was not attempted.

Temperature-Programmed Oxidation (TPO) of carbonaceous deposits was carried out in a quartz microreactor coupled to a quadrupole residual gas analyzer from MKS (PPT 4.24). The TPO experiments were used to determine the amount of carbon that was deposited under reaction conditions. These experiments were also used to provide information about the location of the carbon. After reaction the samples were cooled to room temperature in He and then heated up to 1073 K at a rate of 8 K/min in a 5% O₂/He mixture (30 cm³/min). After the system reached 1073 K, pulses containing 100 μL of CO₂ were injected, and the peak areas were used to quantify the amount of carbon formed on the catalyst.

Pulse experiments using CH₄ and CO₂ were performed in the same reactor system as previously described using 10 mg of catalyst. The samples were heated to 773 K in hydrogen (30 cm³/min) and reduced *in situ* for 1 h. After reduction, the samples were heated to 1073 K in He (15 cm³/min) and, while in He, exposed to pulses of CH₄, CO₂, or mixtures of the reactants (50 μL pulses, 10–15 min apart). During each pulse the exit gases were analyzed using the quadrupole residual gas analyzer. The area of each pulse was converted to moles using a conversion factor that was determined from a calibrated injection prior to the experiments.

X-ray diffraction experiments were carried out on a Rigaku Automatic Diffractometer (Model D-MAX A) with a curved crystal monochromator and system setting of 40 kV and 30 mA. Data were collected in the angle range of 5.0° to 70.0° with a step size of 0.05° and a count time of 1.0 s. The samples were finely ground and then placed on the glass slide using a smear mount technique. TEM was performed on a JEOL 2000FX TEM. After the catalyst was exposed to the specific pretreatment, reduction, or reaction, the sample was then ground into a fine powder and suspended in isopropyl alcohol. One drop of solution was placed on a 0.3-mm-diameter Lacey carbon grid (Electron Microscopy Sciences) and allowed to dry. The physical properties of the materials were obtained using a Micromeritics ASAP 2010 adsorption apparatus. All of the samples were degassed for approximately 20 h before the experiments were started.

Extended X-ray Absorption Fine Structure (EXAFS) and X-ray Absorption Near Edge Spectroscopy (XANES) were performed on beamlines X-18B and X-23A2 at the National Synchrotron Light Source at Brookhaven National Laboratory, Upton, New York. The ring energy was 2.5 GeV with a ring current of 80–220 mA. An Si(111) and Si(100) crystal monochromator was used to vary the photon energy incident to the sample. The spectra were recorded near the L_{III} -edge of Pt (11,564 eV) and the K-edge for Sn (29,200 eV) ranging from 50 eV below the edge to at least 1000 eV past the edge. For each sample, the optimum mixture of catalyst and diluent ($\text{SiO}_2/\text{ZrO}_2$) was determined, thoroughly mixed, and then pressed into pellets. EXAFS experiments were performed on samples that had been prepared in our laboratory. After exposure to reaction at 1073 K, the pellets were then transferred to a glove bag filled with He and sealed into holders with Kapton tape without exposure to air. The samples were then placed into a stainless-steel cell, which could be cooled to liquid nitrogen temperatures. EXAFS spectra on the reduced samples and those samples exposed to reaction conditions were recorded at liquid nitrogen temperatures. A theoretical reference for the Pt–Pt bond was obtained by using the FEFF program from the University of Washington (32–34). The FEFFIT fitting routine was employed to obtain the structural parameters of the Pt clusters after the various pretreatments and reactions. The variables that were used in the fitting included the Debye Waller factor (σ), the edge energy difference (ΔE_0), the coordination number (N), and the difference in the bond distances (ΔR) with respect to the theoretical bond distance.

RESULTS

Catalytic Activity in the Flow System

Table 1 contains the CH_4 and CO_2 fractional conversion for the Pt/ ZrO_2 , Pt/Ce– ZrO_2 (5 wt%), Pt/Ce– ZrO_2 (18 wt%), and the Pt/La– ZrO_2 after 5, 400, 800, and

TABLE 1
 CH_4 and CO_2 Conversion during 23 h of Reaction at 1073 K with a CH_4 : CO_2 Ratio of 2 : 1

Time on stream (min)	CH_4 % conversion				CO_2 % conversion			
	5	400	800	1200	5	400	800	1200
Pt/ ZrO_2	18	15	14	13	33	27	25	23
Pt/La– ZrO_2	26	25	25	25	37	33	30	30
Pt/Ce– ZrO_2 5 wt%	21	18	16	16	35	31	29	29
Pt/Ce– ZrO_2 18 wt%	17	18	19	19	33	35	35	35

1,200 min of reaction at 1073 K and a 2 : 1 CH_4 : CO_2 feed ratio. As mentioned above, these conditions are much more severe than those in most studies reported in the literature (4). Under these conditions, the La-promoted catalyst exhibited higher initial CH_4 and CO_2 conversion than the unpromoted and Ce-promoted catalysts. While the conversion of CH_4 on the La-promoted catalyst was constant over the 21 h of reaction, the conversion of CO_2 decreased by almost 20% during the reaction period. The Ce-promoted catalyst (18 wt%) had an initial activity that was equal to that of the unpromoted catalyst; however, unlike the Pt/ ZrO_2 sample, no deactivation was observed on the Pt/Ce– ZrO_2 catalyst. Decreasing the loading of Ce resulted in a slight increase in initial activity but a loss in stability. The conversions were in all cases kept well below the equilibrium conversions, which under these conditions were close to 100% for CO_2 and 50% for CH_4 .

CH_4 and CO_2 Pulse Experiments

Pulse experiments were performed on the Pt/ ZrO_2 catalyst at 1073 K to investigate the effects of the individual reactants and to further develop the proposed cleaning mechanism. Figure 1 shows the H_2 and CO produced during pulses of $\text{CH}_4 + \text{CO}_2$ at a 2 : 1 ratio, CH_4 alone, and CO_2 alone. Pulses of the reaction mixture are shown in panels A, C, and E. Panel B shows the pulses, which contained only CO_2 , while panel D shows the pulses of CH_4 . During

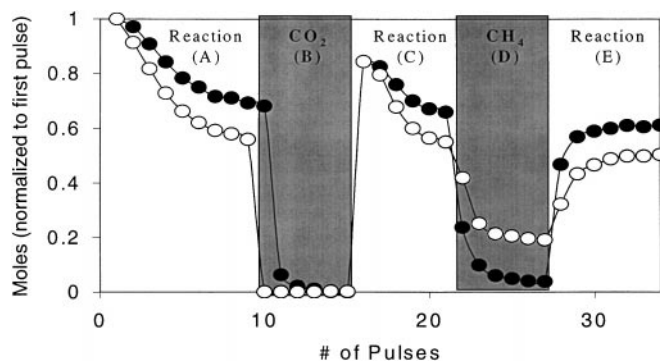


FIG. 1. CO (●) and H_2 (○) production from pulses of reaction mixture (2 : 1 CH_4 : CO_2 ratio), CH_4 , or CO_2 over Pt/ ZrO_2 at 1073 K.

the first set of pulses containing reaction mixture (panel A), the production of CO and H₂ was approximately 1 : 1 for the first pulse, but then it decreased with each subsequent pulse due to carbon deposition on the catalyst. In the subsequent series of CO₂ pulses (panel B) a substantial amount of CO was produced during the first pulse, while the last five pulses of CO₂ resulted in minimal CO production.

The first pulse in the second set of pulses containing the reaction mixture (panel C) again resulted in an equal production of H₂ and CO. More importantly, the amount of CO and H₂ produced during this pulse was greater than the amount produced during the final pulse of the initial reaction series (panel A). This shows that after the series of CO₂ pulses the catalyst regained some of the active sites, indicating that cleaning of the metal particle occurred. Again the amount of CO₂ and H₂ decreased during the subsequent pulses of reaction mixture.

The series of pulses containing pure CH₄ (illustrated in panel D) resulted in the production of both H₂ and CO. It should be noted that the time between individual pulses was 15 min, which is sufficient to flush any remaining oxygen-containing species, present in the gas phase, out of the system. Therefore, the only source of oxygen in the system is from the support. Each CH₄ pulse resulted in less H₂ and CO production than the previous pulse, due to coke deposition. After the series of CH₄ pulses, the third series of reaction pulses (panel E) was sent to the reactor. The initial H₂ and CO production were lower than those in the final pulse of the second series (panel C), but then they increased with each pulse, approaching the production from the last series of reaction pulses (panel C).

Pulse experiments were also performed on the Pt/ZrO₂, Pt/Ce-ZrO₂ (5 wt%), and Pt/La-ZrO₂ catalysts in which the catalysts were reduced at 773 K for 1 h and then exposed to pulses containing either CH₄ or CO₂ at 1073 K. Figure 2a shows the H₂ production during three sets of these pulses. During the first set of CH₄ pulses, the promoted catalysts produced a significant amount of H₂. The amount of H₂ produced for both the La- and the Ce-doped catalysts was approximately 30% more than the amount of H₂ produced on the unpromoted sample, suggesting that the amount of metal exposed for reaction is higher on the promoted samples than on the unpromoted catalyst. As expected, no H₂ was produced during the pulses of CO₂, but this series had the important effect of removing carbon from the metal surface. The effects of the removal of carbon are observed in the subsequent set of CH₄ pulses. The Pt/La-ZrO₂ and Pt/Ce-ZrO₂ (5 wt%) catalysts displayed approximately the same H₂ production that was observed during the first set of CH₄ pulses. The H₂ production on the Pt/ZrO₂ decreased in comparison to the first series, indicating only a partial removal of carbon from the surface of the metal.

Figure 2b is a graph of the CO production in the same set of pulses. During the first series of CH₄ pulses, CO pro-

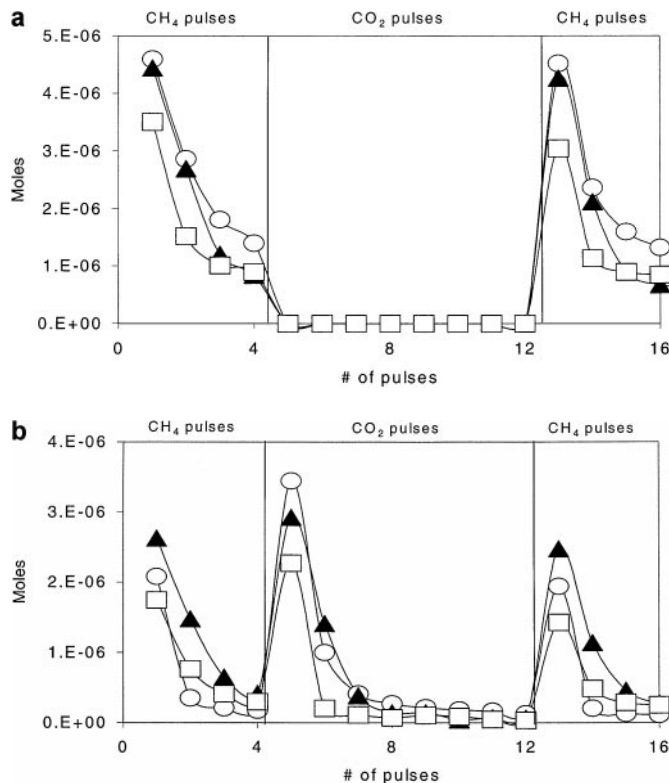


FIG. 2. (a) H₂ production during pulses of either CH₄ or CO₂ at 800°C over the Pt/ZrO₂ (□), Pt/Ce-ZrO₂ (▲), and Pt/La-ZrO₂ (○) catalysts. (b) CO production during pulses of either CH₄ or CO₂ at 1073 K over the Pt/ZrO₂ (□), Pt/Ce-ZrO₂ (▲), and Pt/La-ZrO₂ (○) catalysts.

duction was observed, with the amount of CO decreasing in the order Ce-doped > La-doped > unpromoted catalyst. As mentioned above, there is no oxygen gas-phase species present on the system, which indicates that the oxygen is coming from the support. The following series of pulses contained CO₂. Again, CO was observed on all three catalysts; however, the order of the amount of CO produced changed. Unlike the order during the CH₄ pulses, the La-doped catalyst produced the most CO by CO₂ dissociation, followed by the Ce-promoted sample and then the unpromoted sample. In addition, the La- and Ce-doped catalysts produced CO during the first three pulses in this series, while on the unpromoted sample CO production ceased after the first pulse. During the last series of CH₄ pulses CO was produced again, indicating that the support oxygen was partially replenished during the previous CO₂ pulse series.

Similar to the H₂ production during the CH₄ pulses, the promoted catalysts showed an equivalent production of CO during the two sets of CH₄ pulses, while the CO production on the unpromoted Pt/ZrO₂ decreased from that observed during the first set of pulses. Analysis of the product ratio formed during the pulses of CH₄ can reveal information about the interaction between the metal and the support. Three different situations are possible. If the H₂/CO ratio

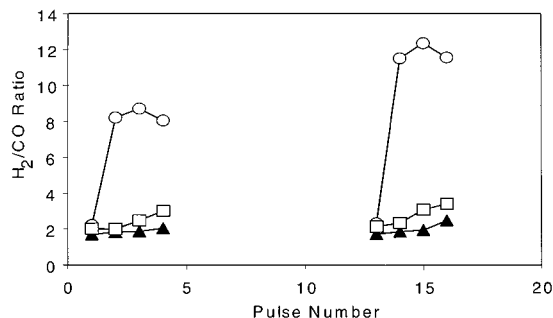


FIG. 3. H_2/CO product ratio for pulses of CH_4 at 1073 K over the Pt/ZrO_2 (\square), $\text{Pt}/\text{Ce-ZrO}_2$ (\blacktriangle), and $\text{Pt}/\text{La-ZrO}_2$ (\circ) catalysts.

was equal to 2, this indicates that during the decomposition of CH_4 , 2 H_2 and 1 CO were formed. A product ratio of 2 indicates that no carbon was left on the catalyst; instead all the carbon used oxygen from the support near the perimeter of the metal particle and formed CO . If the ratio is less than 2, this indicates that a combination of CO , H_2 , and H_2O is being formed. This would occur when the Pt particle is preoxidized and H_2O is formed as a result of the reduction of the metal. Finally, if the H_2/CO ratio is greater than 2, this indicates that carbon is being left on the catalyst. This situation arises through two possible phenomena, (a) minimal reduction of the support occurs and the carbon remains on the metal, and (b) CO (or CO_2) is formed by partial reduction of the support, but it is trapped on the surface. Figure 3 shows the H_2/CO production ratio observed for the same series of CH_4 and CO_2 pulses described for Fig. 2. As no H_2 was observed during the CO_2 pulses, no ratio is reported for this set. The H_2/CO product ratio remained constant at approximately 2 for all of the CH_4 pulses over the $\text{Pt}/\text{Ce-ZrO}_2$ (5 wt%) and Pt/ZrO_2 catalysts. In contrast, the product ratio was 2 for the $\text{Pt}/\text{La-ZrO}_2$ catalyst only for the first pulse in each set. The second pulse of CH_4 results in a product ratio of 8 for the first set and 11 for the second set. This high ratio was then observed for each of the subsequent pulses in the specific set, indicating carbon consumption.

Figure 4 shows the CO production for pulses of either CO_2 or CH_4 over the $\text{Pt}/\text{La-ZrO}_2$ catalyst. The experimen-

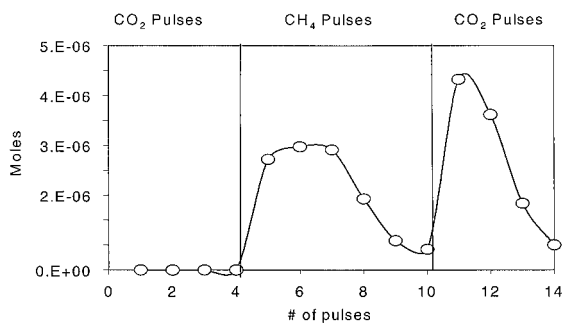


FIG. 4. CO production during pulses of either CO_2 or CH_4 at 1073 K over the $\text{Pt}/\text{La-ZrO}_2$ catalyst.

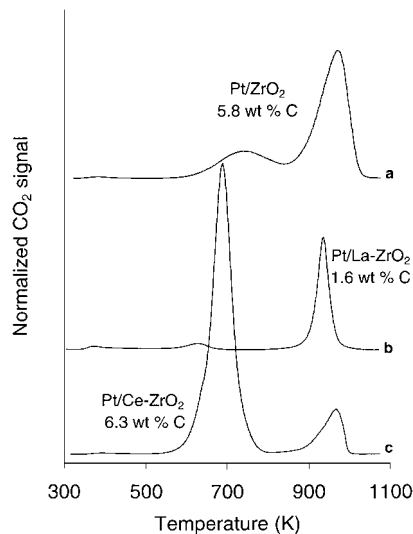


FIG. 5. CO_2 signal during TPO analysis after 23 h of CO_2 reforming of CH_4 reaction at 1073 K with a $\text{CH}_4:\text{CO}_2$ ratio of 2:1: (a) Pt/ZrO_2 , (b) $\text{Pt}/\text{La-ZrO}_2$, (c) $\text{Pt}/\text{Ce-ZrO}_2$.

tal setup was the same as for the previous set of pulses; however, the order of the pulses was reversed. In this experiment, pulses of CO_2 were sent to the reactor first for the purpose of probing the role of the vacancies. We intended to see if the oxygen vacancies were necessary for the dissociation of CO_2 on the promoted catalyst, as was shown to be the case for the unpromoted sample. As is clearly shown in Fig. 4, no CO was observed during the first set of CO_2 pulses. However, after the pulses of CH_4 caused the partial reduction of the support, the subsequent CO_2 pulses resulted in a significant amount of CO produced.

Temperature-Programmed Oxidation (TPO) of Carbon Deposits

Figure 5 shows the profiles for the TPO of carbon deposits on the Pt/ZrO_2 , $\text{Pt}/\text{La-ZrO}_2$, and $\text{Pt}/\text{Ce-ZrO}_2$ (18 wt%) after 22 h of reaction at 1073 K and a $\text{CH}_4:\text{CO}_2$ ratio of 2:1. The profile for the unpromoted Pt/ZrO_2 catalyst showed a small broad peak centered at around 738 K and a major one at 970 K. Interestingly, while on the unpromoted catalyst the high-temperature peak was dominant, on the Ce-promoted catalyst this peak was very small, while most of the carbon was oxidized at 687 K. The La-promoted catalyst exhibited a very small peak in the low-temperature region and a larger one at very high temperatures, which, as described in the discussion, might be due to decomposition of carbonates formed on the support rather than coke deposits. Overall, the La-promoted catalyst was the one that formed the least amount of coke. On the other hand, the Ce-promoted catalyst does not show a decrease in the amount of carbon formation, but it does show an enhanced ability to eliminate coke at low temperatures.

TABLE 2

Structural Parameters Determined from EXAFS Analysis of Pt/ZrO₂ and Pt/LaZrO₂ Catalysts after Reduction at 500 for 1 h and Reaction at 1073 K with a 3 : 1 CH₄ : CO₂ Ratio

Catalyst	Treatment	<i>N</i> (±0.5)	<i>R</i> (Å) (±0.01)	σ^2 (Å) ² (±0.001)	ΔE_0 (eV) (±1.0)
Pt/ZrO ₂	Reduced	5	2.71	0.0024	-1
Pt/ZrO ₂	Reaction @ 800	10.5	2.69	0.0015	-7
Pt/La-ZrO ₂	Reduced	8.5	2.73	0.0026	4
Pt/La-ZrO ₂	Reaction @ 800	9.4	2.72	0.002	5

X-Ray Diffraction

XRD was performed on the Pt/ZrO₂, Pt/Ce-ZrO₂ (5 wt%), Pt/Ce-ZrO₂ (18 wt%), and Pt/La-ZrO₂ catalysts after calcination at 1073 K for 4 h. After this treatment, the ZrO₂ in the unpromoted sample consisted primarily of the monoclinic phase, while the La-doped and Ce-doped (18 wt%) sample were completely tetragonal. The Ce-doped (5 wt%) sample showed evidence of both monoclinic and tetragonal phases.

Characterization of the Supported Metal Particles

EXAFS studies were performed on the Pt/ZrO₂, Pt/Ce-ZrO₂ (5 wt%), and Pt/La-ZrO₂ catalysts to determine if the presence of the promoters had any effect in inhibiting or accelerating particle growth under reaction conditions. The Fourier Transform (FT) of the EXAFS data corresponding to reduced fresh samples and samples exposed to reaction at 1073 K have been reported elsewhere (21). Table 2 shows the results of the fitting of these EXAFS data, obtained for the Pt/ZrO₂ and Pt/LaZrO₂ catalysts after reduction at 773 K for 1 h and after 1073 K reaction at a 3 : 1 CH₄ : CO₂ ratio. The data show that the fresh La-promoted catalyst had larger particles than the unpromoted Pt/ZrO₂ catalyst, with a coordination number of approximately 8.5 compared to 5 for the unpromoted catalyst. However, after reaction at 1073 K the unpromoted catalysts exhibited more sintering with a final coordination number of 10.5, while the La-promoted catalyst coordination number only increased slightly to 9.4. Based on the coordination numbers obtained from EXAFS, assuming cubo-octahedral crystallites of FCC structure, the metal particle size can be estimated (35). Accordingly, the Pt/ZrO₂ catalyst, which showed the greatest loss of activity during the first 2 h on stream, had an average particle diameter of 0.7 nm after reduction at 773 K, but it grew to a diameter of 3.2 nm after reaction at 1073 K. Conversely, the La-doped catalysts, which had increased stability, exhibited only minimal particle growth, with the diameter of the Pt particles increasing from 1.3 nm after reduction at 773 K to 1.9 nm after reaction at 1073 K.

The particle size estimation from the EXAFS data has been used to calculate the metal dispersion (fraction of

metal exposed) and, consequently, the turnover frequency (TOF) for the La-promoted and unpromoted catalysts, based on the conversion of CH₄. Accordingly, the metal dispersion was calculated based on the well-known relationship for Pt, $D(\%) = 113/d$ (nm) (18). The CH₄ TOF for the unpromoted catalyst was initially high at 0.51 s⁻¹, but over the course of the 22-h reaction it dropped significantly to 0.37 s⁻¹. Conversely, the CH₄ TOF for the La-promoted catalyst was initially lower than that for the unpromoted ZrO₂ catalyst at 0.44 s⁻¹, but it only dropped to 0.42 s⁻¹ over the 22-h reaction period.

DISCUSSION

The results presented in this paper show that the addition of either Ce or La oxide results in improved catalytic performance for the reforming of methane by CO₂. Both of the individually promoted catalysts exhibited higher stability than the Pt/ZrO₂ catalyst. The promotional effects of the lanthanum may stem from its ability to increase the thermal stability of the support, while the cerium is successful at increasing the oxygen exchange capacity of the support. These two promoting effects have been observed for La and Ce in other reaction systems (23, 24, 31). Previous work performed by our group using isotopically labeled molecules has shown that the support has a strong effect on the activity and stability of the catalyst (20). In those studies, when the unpromoted Pt/ZrO₂ catalyst was exposed to pulses of ¹³CH₄, formation of ¹³CO, together with small amounts of ¹³CO₂, was observed. X-ray absorption studies demonstrated that the metal particles were completely reduced. Therefore, the only possible source of oxygen in this experiment was the support. It was then suggested that some of the carbon produced from the decomposition of ¹³CH₄ partially reduced the oxide support near the perimeter of the particle. The remaining ¹³C produced from the decomposition of ¹³CH₄ was deposited on the Pt metal, possibly as ¹³CH_x species. Subsequent pulses of ¹²CO₂ pulses resulted in the production of both ¹²CO and ¹³CO, which supported the idea that carbon was removed from the metal particles under reaction conditions. The results also showed that Pt is needed to catalyze the dissociation of CO₂. Consequently, either the dissociation takes place near the metal-support interface or it occurs on oxygen vacancies generated during the previous reduction of the support by the methane pulses. These results supported the two-path mechanism for the CO₂ reforming of CH₄ previously described (20). The first path involves the decomposition of CH₄ on the metal particle, resulting in the formation of H₂ and carbon, which can either partially reduce the oxide support near the metal particle or, in the absence of a reducible oxide, form carbon deposits on the metal. The second path is the dissociation of CO₂. The CO₂ adsorbs on the support and, near the metal particle, it dissociates to form CO and O. The oxygen

formed during the dissociation can then reoxidize the support to provide a redox mechanism for continuous cleaning. The balance between the rate of decomposition and the rate of cleaning determines the overall stability of the catalyst. This mechanism is similar to that proposed by other groups working at lower temperatures (873 K) (18, 36). The main difference between this mechanism and those at lower temperatures is the absence of the formation of hydroxyl groups on the support at high temperatures, where it is unlikely that, at 1073 K, hydroxyl species would be present on the surface of the catalyst.

The reaction pulse experiments presented in Fig. 1 provide further evidence for the balance between the rate of cleaning and the rate of deposition determining the long-term activity of the catalyst. During all three reaction-pulse series, the production of H₂ and CO for the final pulse approached the same value. More importantly, the production of H₂ and CO increased with each subsequent pulse in the last set of pulses. This can be explained by considering the state of the metal particle surface and the surrounding support after the pulses of CH₄ without any CO₂ present.

It can be expected that after this series (panel D), the metal particles should have a significant amount of carbon deposits, while the support near the perimeter of the particle should exhibit a relatively high density of oxygen vacancies. The coke on the metal particle inhibits the decomposition of methane, by physically blocking metal sites. However, the support near the metal particle is sufficiently reduced to facilitate the adsorption and dissociation of CO₂, which then allows for the cleaning of the metal particle by oxidation of the carbon on the metal surface. As a result, each pulse in panel E results in gradually increasing activity until the cleaning rate and the rate of CH₄ decomposition come into balance. Thus, promoters with the ability to further enhance the dissociation of CO₂, oxygen exchange, and removal of carbon from the metal should result in improved catalytic performance.

Lanthanum Promotion

Unlike the Ce-doped and unpromoted samples, the La-doped catalyst exhibited a strong tendency for carbon retention in the absence of CO₂ (Fig. 3) with the H₂/CO ratio increasing drastically after the first pulse of CH₄. As stated in the results, the high ratio can be due to either carbon formation or CO/CO₂ retention on the surface via the formation of carbonate species. The fact that the first pulse of CH₄ resulted in an H₂:CO ratio of 2 indicates that reduction of the support was occurring and no CO was being trapped on the surface as a carbonate species. Others have observed that on rare-earth oxides increased reduction results in an inhibition of carbonate-like species from CO at room temperature (37). It is highly unlikely that subsequent pulses would result in trapping of carbon by the support.

The temperature-programmed oxidation studies show that after reaction the La-promoted catalyst has less carbon than either the Ce-promoted or the unpromoted ZrO₂ catalyst. Clearly, the lanthanum must have promotional effects *in the presence of CO₂*, which result in improved stability for the dry reforming reaction.

One explanation for the higher activity and stability of the La-promoted catalyst is that the addition of La results in increased thermal stability and a resultant increase in the surface area after calcination at 1073 K. XRD diffraction studies of the La-promoted ZrO₂ demonstrated the ability of the La to stabilize the tetragonal phase of ZrO₂ and increase the surface area over 1.5 times that of the ZrO₂ and Ce-promoted supports. This increase in the thermal stability can have several beneficial effects. Due to the basicity of the support, this increase in surface area can result in an increase in the CO₂ adsorption capacity. Zhang and co-workers have suggested that catalysts composed of Ni supported on La₂O₃ had higher stability compared to Al₂O₃- and CaO-supported Ni catalysts due to the ability of the La₂O₃ to activate the CO₂ in the form of carbonates (38). It is possible that the addition of La to ZrO₂ has a similar effect. Lercher and co-workers (39) suggested that at 873 K, carbonate species were formed on a Pt/ZrO₂ catalyst and that the carbonate interacted with the carbon on the metal surface to form CO and a formate species. The formate species then decomposed to form a hydroxyl species and CO. As stated before, it is unlikely that hydroxyl species would be adsorbed on the surface of the catalyst at 1073 K. Thus, the mechanism of the reaction at 1073 K must be different than those mechanisms previously reported.

The results presented in Fig. 4 provide support for the formation of carbonate species as well as the role of the oxygen vacancies in the activation of CO₂ on the La-promoted catalyst. Pulses of CO₂ over a fresh catalyst showed that no CO species were formed. This indicates that no dissociation of CO₂ is occurring. It is likely that carbonate species were being formed on the surface of the catalyst during these pulses but that the presence of the reduced metal alone was not sufficient for dissociation to occur. The subsequent pulses of CH₄ resulted in the production of CO. These pulses combined with the pulse experiments shown in Fig. 2b can provide some insight as to the origin of the CO formed during CH₄ pulses. Figure 2b shows that prior to the formation of carbonate species on the surface, the addition of CH₄ into the system results in the production of CO. As previously discussed, the CO is formed by the carbon from the decomposition of CH₄, partially reducing the support near the metal particle-support interface. It should be noted that the amount of catalyst and the conditions of the pulse experiments shown in Figs. 2b and 4 were the same. It is clear that the amount of CO formed during pulses of CH₄ after exposure to CO₂ is greater than the amount formed prior to CO₂ exposure. It is probable that the additional CO formed is

due to interaction of the carbon with the carbonate species on the support. The importance of the oxygen vacancies formed during the decomposition of CH₄ can also be seen in both pulse studies. After the pulses of CH₄, subsequent CO₂ pulses resulted in the formation of CO, showing that the vacancies are necessary for the activation of CO₂ in the absence of CH₄. Isotopically labeled studies have been previously performed (20), in which it was shown that the CO is produced both from the dissociation of CO₂ and from the removal of carbon that is deposited on the metal particle during the decomposition of CH₄. Therefore it is possible that the carbon formed during the decomposition of CH₄ is acting to reduce the support near the metal particle and activate the carbonate species adsorbed on the support.

Cerium Promotion

The results of the pulse studies combined with DRIFTS experiments reported elsewhere (40) show that the oxygen vacancies formed in the support during the decomposition of CH₄ play an important role in the reaction mechanism (20). The interaction of CH₄ with the catalyst results in the reduction of the support near the metal particle, and it may be at this vacancy site that the adsorption and dissociation of CO₂ occurs. The dissociation of CO₂ results in the production of CO and a replenishing of the oxygen in the lattice. This mechanism has been verified for the promoted catalysts by the pulse studies shown in Fig. 4. CO₂ dissociation did not occur on the Pt/La-ZrO₂ catalyst until after the catalyst was exposed to pulses of CH₄ and the support was partially reduced. Thus, the ability of a promoter to increase the reducibility of the oxide support and/or its oxygen exchange capacity could have a tremendous impact on the stability of the catalyst.

Ceria is known to be a material with high oxygen storage capacity, which can be combined with other solid materials such as ZrO₂ to make a material that promotes the formation of oxygen vacancies and increases the mobility of oxygen through the lattice (26, 41). Furthermore, it has been shown that the surface area of the ceria-zirconia material has no bearing on the reduction properties, such that equivalent degrees of reduction are observed for both high and low surface area materials. For the purpose of this investigation, where high interfacial area between the particle and the support is crucial, we have chosen to dope ZrO₂ with cerium to maintain a high surface area material and achieve a high dispersion of Pt.

The results of this study have shown that the addition of Ce⁴⁺ to the ZrO₂ did improve the reducibility of the oxide and had a beneficial effect on the long-term activity of the catalyst. The H₂/CO ratio reported in Fig. 3 indicates that the support is readily reducible in the presence of a hydrocarbon at high temperatures. During both sets of CH₄ pulses (before and after exposure to CO₂) the Ce-doped catalyst yielded a H₂/CO ratio very near 2, which is the ratio that

one expects if no carbon deposition occurs. The higher reducibility of the support results in an enhanced ability to clean the carbon that would normally accumulate on the metal during the decomposition of CH₄. This cleaning ability is not necessarily reflected in the total amount of carbon deposits observed by TPO. In fact, as shown in Fig. 5, the total amount of carbon left on the Pt/Ce-ZrO₂ after 22 h of reaction at 1073 K and a 2 : 1 CH₄ : CO₂ ratio is about the same as that on the Pt/ZrO₂ sample. However, the ability of the catalyst to eliminate the carbon is clearly superior, as indicated by the lower temperature of oxidation. Similar results have been observed on cerium-oxide-supported Ni catalysts for the steam reforming reaction (42). The low-temperature peaks observed in TPOs of coked Pt/Al₂O₃ catalysts have been typically ascribed to carbon near the metal particles, while those at high temperatures have been ascribed to carbon on the support (43). However, in the case of Pt/Ce-ZrO₂ catalysts, we ascribe this low-temperature TPO peak to carbon that is not immediately near the metal particle, since as indicated by the lack of catalyst deactivation, this carbon is continuously eliminated during reaction.

The promotional effect of Ce⁴⁺ on the oxygen transfer is also shown when the amounts of CO produced from the CH₄ pulses (Fig. 2b) are compared. During the pulses of CH₄, the Ce-doped catalyst produced the most CO, indicating the highest degree of support reduction. A higher degree of reduction results in an increase in the number of oxygen vacancies formed near the metal particle and a subsequent increase in the ability to dissociate CO₂. Results similar to these have recently been obtained on Pd/ceria and Pd/zirconia catalysts (44). Even though the Ce-doped support does not have a higher BET surface area than the ZrO₂ support, the increase in the dissociation ability and subsequent cleaning capacity results in a catalyst with enhanced activity and stability for the CO₂ reforming reaction.

Increasing the loading of Ce in the support from 5 to 18 wt% resulted in a slight decrease in the initial activity of the catalyst but a significant improvement in the stability for the dry reforming reaction. Table 1 shows that no loss in either CH₄ or CO₂ activity was observed on the catalyst with 18 wt% cerium, while some loss of activity was observed on the catalyst with lower loading. XRD studies showed that the higher loading resulted in a complete stabilization of the tetragonal form of ZrO₂. The increased thermal stability of the support is most likely due to the increased stability for the reasons described above. Further studies are being conducted to determine the optimum loading of Ce for the dry reforming reaction.

Metal Particle Size Effects

Another effect of the addition of promoters can be inferred from the EXAFS data. The fitting parameters indicate that although the metallic Pt clusters on the promoted

catalysts were larger than those on the unpromoted catalysts before reaction, they were smaller under reaction conditions. After 2 h of reaction at 1073 K and a 3 : 1 CH₄ : CO₂ ratio, the Pt particles on the unpromoted catalyst were larger than those on either the Ce- or the La-doped catalyst. In fact, the promoted samples exhibited only moderate particle growth. Similar results were also observed using transmission electron microscopy. Comparing the activity of the catalysts with the degree of particle growth observed indicates that the degree of sintering follows the same order as the rate of deactivation.

Based on the proposed importance of the metal-support interface, it is obvious that sintering of the Pt metal would have an important role in the deactivation of the catalyst because it results in a decrease in the metal-support interaction, limiting the removal of carbon from the metal. Furthermore, the amount of carbon required to deactivate the catalyst would be much smaller, and consequently the activity of the catalyst would decrease rapidly.

Figure 2a shows that the hydrogen production during the pulses of CH₄ is much lower on the unpromoted Pt/ZrO₂ catalyst as compared to the promoted samples. It is then possible that sintering is a major contributor to the lower activity and faster rate of deactivation for the Pt/ZrO₂ catalyst at 1073 K. The lower activity can be ascribed to the reduction in the area of active metal exposed for reaction on the Pt/ZrO₂ catalyst. It should be noted that the sintering of the Pt particles most likely occurs during the heating to 1073 K and not under reaction conditions. Figure 2a shows that the promoted catalysts regained nearly 100% of the hydrogen production observed during the first set of CH₄ pulses. If sintering occurred during the reaction, it would be reasonable to observe a decrease in the activity, which could not be regained by exposure to pulses of CO₂. Although the Pt/ZrO₂ did exhibit some loss in initial activity, this loss is most likely due to less efficient cleaning on the unpromoted catalyst, which results in a reduction in the amount of exposed active metal due to carbon formation.

The results of the EXAFS and pulse studies show that agglomeration of the Pt particles does occur when the catalyst is heated to high temperatures. This sintering is detrimental to the activity of the catalyst because it decreases the area of metal exposed for reaction. However, an even greater effect is observed on the stability of the catalyst due to a reduction in the metal-support interaction. A reduction in the interfacial area leads to a reduction in the ability of the catalyst to dissociate CO₂ and an increase in the formation of carbon on the metal. The results of this work have shown that the promoted catalysts do not experience significant sintering. Therefore, the final benefit of the cerium and lanthanum is that their presence retards the Pt particle growth and the role of the support is not hindered at high temperatures, leading to increased stability.

CONCLUSIONS

The results presented in this paper demonstrate that the addition of cerium and lanthanum to the support has several promotional effects. First, the promoters can increase the thermal stability of the catalyst by stabilizing the tetragonal phase of zirconia. This stabilization results in an increase in the surface area and an increase in the density of CO₂ adsorption sites near the metal particle. Based on the two-path mechanism previously described, the ability of the support to enhance the dissociation of CO₂ near the Pt particle and the transfer of oxygen to the coked metal greatly accelerates the cleaning mechanism, resulting in improved stability. Second, the addition of promoters aids in retarding Pt particle growth. This is not only beneficial for increasing the active metal surface exposed for reaction but also maintains a high particle-support interfacial area, which is crucial for efficient cleaning of the metal particle.

REFERENCES

1. Fischer, V. F., and Tropsch, H., *Brennst.-Chem.* **3**, 39 (1928).
2. Gadalla, A. M., and Sommer, M. E., *Chem. Eng. Sci.* **44**, 2825 (1989).
3. Erdohelyi, A., Cserenyi, J., and Solymosi, F., *J. Catal.* **141**, 287 (1993).
4. Ross, J. R. H., van Keulen, A. N. J., Hegarty, M. E. S., and Seshan, K., *Catal. Today* **30**, 193 (1996).
5. Wang, S. B., and Lu, G. Q., *Energy Fuels* **10**, 896 (1996).
6. Choudhary, V. R., and Rajput, A. M., *Ind. Eng. Chem. Res.* **35**, 3934 (1996).
7. Xiaoding, X., and Moulijn, J. A., *Energy Fuels* **10**, 305 (1996).
8. Qin, D., and Lapszewicz, J., *Catal. Today* **21**, 551 (1994).
9. Zhang, Z. L., and Verykios, X. E., *Appl. Catal. A* **133**, 109 (1996).
10. "The Shell Review," Shell International Petroleum Company Limited, 1994.
11. Takano, A., Tagawa, T., and Goto, S., *J. Chem. Eng. Jpn.* **27**, 727 (1994).
12. Solymosi, F., Kustan, G., and Erdohelyi, A., *Catal. Lett.* **11**, 149 (1991).
13. Zhang, Z. L., Tspouriari, V. A., Efstathiou, A. M., and Verykios, X. E., *J. Catal.* **158**, 51 (1996).
14. Stagg, S. M., and Resasco, D. E., *Stud. Surf. Sci. Catal.* **111**, 543 (1997).
15. Lercher, J. A., Bitter, J. H., Hally, W., Niessen, W., and Seshan, K., *Stud. Surf. Sci. Catal.* **101**, 463 (1996).
16. Hally, W., Bitter, J. H., Seshan, K., Lercher, J. A., and Ross, J. R. H., *Stud. Surf. Sci. Catal.* **88**, 167 (1994).
17. Bitter, J. H., Seshan, K., and Lercher, J. A., *J. Catal.* **171**, 279 (1997).
18. Bradford, M., and Vannice, M. A., *J. Catal.* **173**, 157 (1998).
19. Bradford, M., and Vannice, M. A., *Catal. Lett.* **48**, 31 (1997).
20. Stagg, S. M., Romero, E., Padro, C., and Resasco, D. E., *J. Catal.* **178**, 137 (1998).
21. Stagg, S. M., and Resasco, D. E., *Stud. Surf. Sci. Catal.* **119**, 813 (1998).
22. Ross, J. R. H., Seshan, K., Erzeng, X., and Mercera, P. D., German Patent DE 94 00 513, 1994.
23. Duchet, J. C., Tilliette, M. J., and Cornet, D., *Catal. Today* **10**, 507 (1991).
24. Morterra, C., Cerrato, G., and Ferroni, L., *J. Chem. Soc. Faraday Trans.* **91**, 125 (1995).
25. Blom, R., Dahl, I. M., Slagtern, A., Sortland, B., Spjelkavik, A., and Tangstad, E., *Catal. Today* **21**, 535 (1994).
26. Trovarelli, A., de Leitenburg, C., and Dolcetti, G., *Chemtech* **27**, 32 (1997).
27. Tsukuma, K., and Shimada, M., *J. Mater. Sci.* **10**, 1178 (1985).
28. Sato, T., and Shimada, M., *Am. Ceram. Soc. Bull.* **64**, 1382 (1985).

29. Fornasiero, P., Balducci, G., Di Monte, R., Kaspar, J., Meriani, S., Trovarelli, A., and Graziani, M., *J. Catal.* **151**, 168 (1995).
30. Fornasiero, P., Kaspar, and Graziani, M., *J. Catal.* **167**, 567 (1997).
31. Balducci, G., Fornasiero, P., Di Monte, R., Kaspar, J., Meriani, S., and Graziani, M., *Catal. Lett.* **164**, 173 (1996).
32. Rehr, J. J., Zabinsky, S. I., and Albers, R. C., *Phys. Rev. Lett.* **69**, 3397 (1992).
33. Rehr, J. J., Mustre de Leon, J., Zabinsky, S. I., and Albers, R. C., *J. Am. Chem. Soc.* **113**, 5135 (1991).
34. Mustre de Leon, J., Rehr, J. J., Zabinsky, S. I., and Albers, R. C., *Phys. Rev. B* **44**, 4146 (1991).
35. Gates, B. C., Katzer, J. R., and Schuit, G. C. A., in "Chemistry of Catalytic Processes," p. 246. McGraw-Hill, New York, 1979.
36. O'Conner, A. M., Meunier, F. C., and Ross, J. R. H., *Stud. Surf. Sci. Catal.* **119**, 819 (1998).
37. Sakata, Y., Arai, T., Domen, K., Maruya, K., and Onishi, T., *J. Chem. Soc. Faraday Trans. 1* **85**(6), 1451 (1989).
38. Zhang, Z., Verykios, X. E., MacDonald, S. M., and Affrossman, S., *J. Phys. Chem.* **100**, 744 (1996).
39. Bitter, J. H., Seshan, K., and Lercher, J. A., *J. Catal.* **176**, 93 (1998).
40. Stagg-Williams, S. M., Soares, R., Romero, E., Alvarez, W. E., and Resasco, D. E., *Stud. Surf. Sci. Catal.*, in press.
41. Yao, M. H., Baird, R. J., Kunz, F. W., and Hoost, T. E., *J. Catal.* **166**, 67 (1997).
42. Zhuang, Q., Qin, Y., and Chang, L., *Appl. Catal.* **70**, 1 (1991).
43. Bacaud, R., Charcosset, H., Guemin, M., Torresea-Hidalgo, H., and Tournayan, L., *Appl. Catal.* **1**, 81 (1981).
44. Sharma, S., Hilaire, S., Vohs, J. M., Gorte, R. J., and Jen, H. W., *J. Catal.* **190**, 199 (2000).